Quartz capillary flow meter for gases

Robert F. Berg[a)]
Process Measurements Division, National Institute of Standards and Technology, Gaithersburg, Maryland 20899-8364

(Received 26 September 2003; accepted 24 November 2003)

This article describes an accurate meter for gas flow rates below 1000 μmol/s. (1 μmol/s≅1.3 cm^3/min at 0 °C and 1 atm). Two gauges measure the input and output pressures as the gas flows through a flow element consisting of either a single quartz capillary or an array of parallel quartz capillaries. A hydrodynamic model determines the molar flow rate from the two pressures, the gas temperature, and the gas properties. Measurements with nitrogen demonstrated that three flow elements could span the flow range from 0.1 to 1000 μmol/s with a standard uncertainty of less than 0.03%. Additional measurements with helium, argon, propane, and sulfur hexafluoride demonstrated that, by using the capillary radius determined for nitrogen, the model could predict the flow rates of gases with widely varying properties. [DOI: 10.1063/1.1642751]

I. INTRODUCTION

This article describes a quartz capillary flow meter (QCFM) for gas flow rates below 1000 μmol/s. The QCFM comprises a long quartz capillary, two pressure transducers, and two thermometers. The pressure transducers measure the input and output pressures of the capillary: P_1 and P_2. A hydrodynamic model determines the flow rate to an uncertainty of 0.03% from P_1, P_2, the temperature T, and the gas properties.

The QCFM is a portable transfer standard that compares primary flow meters at the National Institute of Standards and Technology (NIST) to those elsewhere. (For example, see Ref. 1.) Gas flow comparisons are especially useful for the semiconductor electronics industry, which uses thermal mass flow meters to control processes such as plasma etching. The large diversity of the process gases challenges the companies that manufacture and calibrate thermal mass flow meters; the QCFM can handle such diversity.

Figure 1 compares the QCFM with two primary flow meters. The comparisons were made with nitrogen during an interval of 2 years. For larger flows the primary meter was usually a static gravimetric method (weighing the gas supply bottle before and after the flow comparison). For smaller flows the primary meter was usually a $PVTt$ technique (measurements of pressure, volume, temperature, and time in a constant-pressure bellows flow meter). The primary flow meters are described in detail elsewhere;[2] their reproducibilities are comparable to that of the QCFM. Spanning the range from 0.1 to 1000 μmol/s required three flow elements designed for small (No. 7), medium (No. 5), and large (No. 6) flow rates (see Table I). Each flow element comprised either a single capillary or an array of parallel capillaries, and the value for its average capillary radius R was chosen to minimize the deviations shown in Fig. 1.

Figure 2 shows the results for five gases flowing through the medium element. The value $R=0.156\,925$ mm, which was used for all five gases, minimizes the deviations for nitrogen. The deviations for the other gases have flow-independent offsets that are within the uncertainties of the published viscosity values used in the hydrodynamic model.

With the exception of helium, the model required no other adjustable parameter. (The momentum accommodation coefficient for helium was determined from additional measurements.) The need for only one parameter simplified the design and calibration of the QCFM, and it enabled faster diagnoses of problems caused by, for example, inaccurate pressure readings. Furthermore, calibrating the QCFM with, for example, nitrogen, calibrated it for other gases.

The nitrogen calibration was the best way to determine the effective capillary radius. An accurate determination of R by other means would have increased the QCFM uncertainty to that of the viscosity of nitrogen. It bears emphasis that

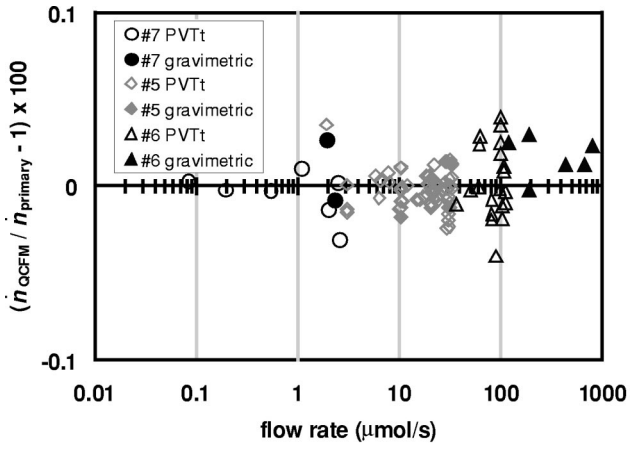

FIG. 1. Deviations of the nitrogen flow rate indicated in the three flow elements (see Table I) from the flow rate measured with a $PVTt$ standard (open points) and a gravimetric standard (solid points). Capillaries Nos. 7, 5, and 6 were designed, respectively, for small, medium, and large flow rates (see Table I).

a)Electronic mail: robert.berg@nist.gov

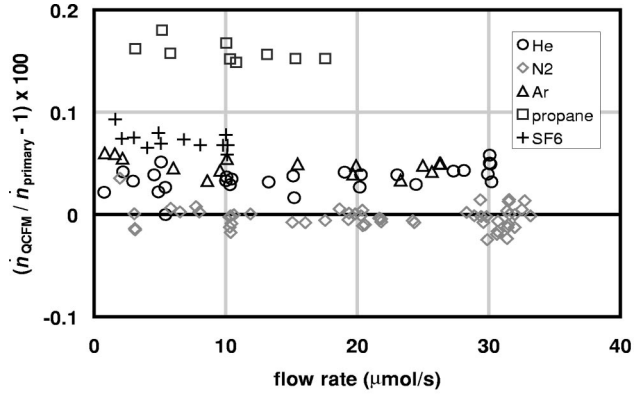

FIG. 2. Normalized deviations of the indicated flow rate in the medium element (No. 5) from that measured with the *PVTt* primary standard. Flow rates for propane and SF_6 with De>16 are not shown. The differences between the five gases are within the uncertainties of published viscosity values.

measurements at multiple flow rates and with other gases are useful for confirming the correct operation of the QCFM.

The QCFM was constructed from commercially purchased capillaries with a circular cross section, which allowed improvements in the hydrodynamic model and simplified the construction of the flow elements. The capillaries have radii that are consistent to within 0.5% for lengths up to 30 m. An earlier NIST transfer standard used a stainless steel, helical duct of rectangular cross section in place of a quartz capillary.[3] Because centrifugal effects are harder to model in a rectangular duct than in a circular duct, the calibration of the earlier standard relied on numerical hydrodynamic calculations, and it required an additional free parameter.

Sections II, III, and IV, respectively, describe the apparatus, operation, and hydrodynamic model of the QCFM. Section V describes the uncertainty of the QCFM, and Sec. VI gives an algorithm for designing a similar flow meter. Reference 4 discusses the derivation of the hydrodynamic model.

II. APPARATUS

A. Air bath and pressure manifold

The QCFM resides in a 15 L air bath made from an insulated picnic cooler that included an internal fan and a thermoelectric heater/cooler (Igloo Kool Cruiser).[5] A temperature sensor and external control electronics were added to achieve a temperature stability of ~10 mK near 25 °C.

TABLE I. Characteristics of the three flow elements.

		Flow element			
		Small (No. 7)	Medium (No. 5)	Large (No. 6)	
Range of flow rate (N_2)	$\dot{n}$	0.07–2.6	0.9–34	55–1900	μmol/s
Capillary inner radius	R	0.1255	0.1569	0.1573	mm
Capillary length	L	33.4	6.4	2.0	m
Radius of curvature	R_{curve}	87	100	100	mm
Capillaries in parallel	N	1	1	19	···
Impedance at small De	L/NR^4	1346	105	2	10^{14} m^3

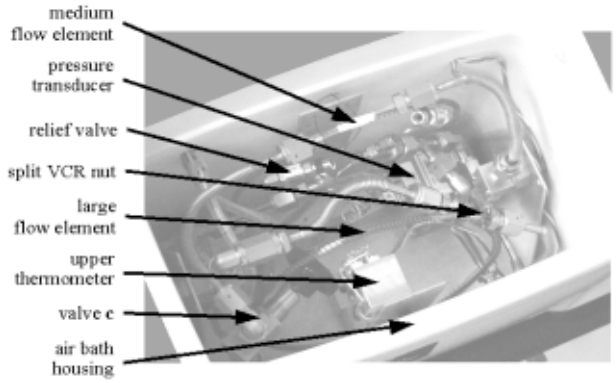

FIG. 3. Interior of the air bath.

(However, the bottom-to-top temperature difference is 0.2 K.) A pressure manifold, two pressure gauges, and two thermometers were bolted to an aluminum frame inside the air bath. The frame could be removed from the air bath to allow easy modifications of the pressure manifold.

Figure 3 shows the interior of the air bath, and Fig. 4 is a schematic diagram of the manifold. Two capillary flow elements can be installed simultaneously in the manifold. Normally, the three manual valves direct the flow through only one of the elements. They were designed for high vacuum service; three-way valves used in an earlier design had intolerable leaks. The handles of valves **a** and **b** protrude through the wall of the air bath to allow switching between elements without opening the air bath. Most of the other components are commercially available stainless steel tees, unions, and bellows tubing having an inside diameter of 4 mm. With the exception of four swaged-ferrule fittings, all of the demountable seals use metal gaskets (Cajon VCR[5]). Particle filters (2 μm) protect the capillaries from dust, and pressure relief valves protect the gauges.

Gas entering the manifold warms from room temperature to the air bath temperature of 25 °C. The characteristic length for the temperature change at small Reynold numbers is $L_T=(2Q_1)/(\pi\beta_1^2 D_T)$, where Q_1 is the volume flow rate, D_T is the thermal diffusivity, and $\beta_1^2=7.3$.[6] For nitrogen flowing at 1000 μmol/s, $L_T=10$ cm, so the 20 cm distance between the entrance filter and the flow element is sufficient.

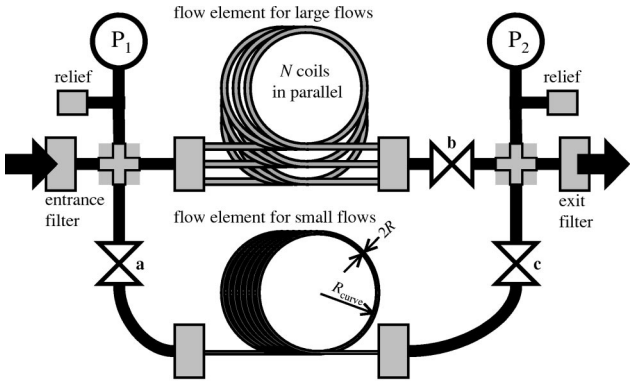

FIG. 4. The manifold includes two flow elements constructed from quartz capillaries. Calibration with nitrogen flow determined the capillary inner radius *R*.

For larger flows, any remaining temperature difference quickly equalizes when the gas is divided among the multiple capillaries of the large flow element (see Table I).

B. Flow elements

The three flow elements were designed to handle flow rates from 0.1 to 1900 μmol/s. Each was assembled from quartz capillary tubing manufactured for gas chromatography (Scientific Glass Engineering).[5] The capillaries were purchased with an untreated inner surface and a polyimide-coated outer surface. The manufacturer specified that the ellipticity was less than 3%, but indicated that the likely value was less than 1%. Radius variations were specified to be less than 0.5%.

For each flow element, the capillary radius R and the length L were chosen to match the maximum flow rate to the range of the input pressure gauge while minimizing the corrections to the hydrodynamic model of the flow element. The value of R was a compromise. A small value of R increased the slip correction, but a large value led to an impracticably long length L, which must increase in proportion to R^4 to maintain a given flow impedance. Section VI describes the design algorithm, and Table I gives the characteristics of the elements.

The medium and small flow elements were assembled by cutting the capillary to the desired length and winding it into a coil with a radius R_{curve} small enough to fit into the air bath. Low-vapor-pressure epoxy was used to glue the capillary ends into blind VCR glands drilled with 1.5 mm diam holes. Short lengths of flexible plastic tubing glued to the capillary insertion points provided strain relief. A loose helix of thin wire wound around the minor diameter of the coil constrained the coil and protected it from abrasion. The large flow element was assembled in a similar manner except that 19 parallel capillaries were used. Dividing the flow among N parallel capillaries reduces the Reynolds number by a factor of N. Coiling the capillary allowed many meters of capillary to be temperature controlled in a small volume, thereby improving the length/radius aspect ratio. A split VCR male nut (split on a bandsaw) fastened the terminating VCR glands to the manifold. Use of a conventional nut would require permanently linking the heavy nut to the fragile capillary. The capillaries were not cleaned.

The effective value of the impedance L/NR^4 was determined by calibration against primary flow standards. Once L/NR^4 was fixed, the values of R, L, and R_{curve} were important only for small corrections in the model. The lengths L of the medium and large flow elements were determined to within 1 mm with a tape measure. The average radius of curvature of the coil R_{curve} was calculated from L and the number of turns N in the coil. The length of the small flow element was determined from the measured value of R_{curve}. Although this method increased the uncertainty of both L and R_{curve}, it avoided unwinding the coil as received from the manufacturer. Both methods determined L and R_{curve} to adequate uncertainty.

Gas diffusion through the quartz walls of the capillary can complicate measurements of helium flow rates. The diffusion was measured by pressurizing the QCFM with helium, closing valves outside the entrance and exit, and observing the time dependence of pressure overnight. The diffusion flow rate was proportional to the helium pressure; at 100 kPa and 25 °C it was approximately 7×10^{-5} μmol/s per meter of capillary. The diffusion was negligible for the medium and large flow elements, and it required only a small correction for the small element. Its uncertainty contribution was therefore negligible.

C. Pressure and temperature transducers

The two pressure gauges are the same model (Paroscientific 6045A[5]) and range (310 kPa full scale). Because the gauges were more than 1 yr old, the manufacturer's uncertainty specification of 0.01% of full scale no longer applied. The exit gauge was recalibrated by comparing it to a third, similar gauge that had been recently calibrated by the Pressure & Vacuum Group at NIST. The entrance gauge was recalibrated by comparing it to the exit gauge at the same pressure. A linear "tare" function $[P_1-P_2=a+b(P_2-100\,\mathrm{kPa})]$ described the apparent difference of the two gauges over the full range. The calibration of the QCFM was maintained by updating the value of a at daily intervals and the value of b at yearly intervals.

The two thermometers are capsule platinum resistance thermometers (PRTs) placed in demountable aluminum blocks. One thermometer was bolted to the bottom of the internal frame and the other to the top. The uncertainty of the temperature measurements is discussed in Sec. V.

D. Electronics

Custom electronics measure the temperature of the air bath and control the power to the thermoelectric heater/cooler. The custom electronics also provide power to the pressure gauges and facilitate their communication with the computer. A digital multimeter measures the four-wire resistance of the two PRTs and communicates with the computer via IEEE-488. The computer periodically records the two pressures and two temperatures. A laptop computer is used for field operation.

III. OPERATION

A. Transportation

The air bath is carried easily by hand. The components necessary for a flow comparison are the flow elements, the air bath (picnic cooler) that holds the pressure manifold, the box containing custom electronics, the digital ohmmeter, and the laptop computer. Before shipping the QCFM by air freight, the flow elements are removed from the pressure manifold, and small pieces of polyethylene foam are jammed inside the air bath to suppress motion of the bellows tubing.

B. Setup and computer control

Preparing the QCFM for use requires installing the flow elements into the air bath, making connections to a gas supply and the flow meter under test, setting up the electronics, flushing out impurities, and waiting for temperature stability.

TABLE II. Corrections (in percent) for flows of 10 μmol/s of helium and sulfur hexafluoride through the medium flow element.

Correction	He	SF_6
virial	−0.07	1.61
slip	0.48	0.05
entrance	−0.00	−0.07
expansion	−0.00	−0.07
thermal	0.00	0.01
centrifugal	0.00	1.61

Because the QCFM uses pressure drops that are large compared to those of many flow meters, it is usually installed upstream of the flow meter under test. Minimizing the volume between the flow meters reduces errors caused by changes of the laboratory temperature.

Viscosity determines the requirement for gas purity. (The filters prevent clogging by dust particles.) For example, a contamination of 2% oxygen in nitrogen increases the viscosity by 0.3%, thereby causing a 0.3% error in the flow measurement. Elimination of air and other contaminating gases requires either evacuation with a vacuum pump or repeated pressure-and-flush cycles.

Achieving a stable temperature distribution inside the air bath requires approximately 2 h. After the temperature is stable, the two pressure transducers are ''tared'' by measuring the apparent difference $P_1 - P_2$ between the transducers at 100 kPa to determine the value of a in the tare function. This is done by isolating the QCFM, opening valves to minimize the impedance between the pressure transducers, and waiting 1 min for pressure equilibrium. A similar procedure at higher pressures gives a sufficient check for leaks. For example, a 10 Pa pressure decrease that occurred at 200 kPa during an interval of 10 min would indicate a leak of approximately 10^{-4} μmol/s.

IV. MODEL OF THE FLOW ELEMENT

The hydrodynamic model for the molar flow rate $\dot{n}$ is

$$\dot{n} = \dot{n}_0 \left[1 + g_{\text{virial}}(P_1, P_2) + 4K_{\text{slip}}\text{Kn} + \frac{K_{\text{ent}}}{16}\frac{R}{L}\text{Re} + \left(\frac{K_{\text{exp}}}{8} + \frac{K_{\text{therm}}}{16} \right) \frac{R}{L}\text{Re}\ln\left(\frac{P_2}{P_1}\right) \right] f_{\text{cent}}\left(\text{De}, \frac{R}{R_{\text{curve}}}\right). \tag{1}$$

The model is implemented in three parts. The first part combines Poiseuille's law and the ideal gas law to approximate the flow through a straight capillary as $\dot{n}_0$. The second part corrects $\dot{n}_0$ for: (a) kinetic energy changes at the capillary entrance, (b) gas expansion along the length of the capillary, (c) viscous heating, (d) slip at the capillary walls, and (e) departures from the ideal gas law. Because the capillary length is much longer than the radius, the first three corrections are small. Operating at an average pressure between 30 and 300 kPa reduces the fourth and fifth corrections. The third part uses the function f_{cent} to correct for centrifugal effects due to coiling the long capillary.

Table II shows example values of the six corrections.

TABLE III. Correction coefficients in the model. The value of K_{slip} does not apply to helium. The value of K_{therm} is for nitrogen; values of K_{therm} for other gases are similar or smaller.

Coefficient	Value	Reference
K_{slip}	+1.00	11
K_{ent}	−1.14	7
K_{exp}	+1.00	8
K_{therm} (N_2)	−0.26	6, this work

Except for slip, all of the corrections are smaller at smaller flow rates. The slip correction for helium through the small flow element can be as large as 1%.

The model is used as a subroutine in the apparatus control program and as a function in an analysis spreadsheet. It must be iterated because most of the corrections depend on the flow rate. The following three subsections describe the model. Reference 4 derives the model.

A. Poiseuille flow of an ideal gas

As a first approximation,[7] the molar flow rate of an ideal gas through a single straight capillary is

$$\dot{n}_0 = \frac{\pi R^4 (P_1^2 - P_2^2)}{16\eta(T,0) L R_{\text{gas}} T}, \tag{2}$$

where R_{gas} is the universal gas constant and $\eta(T,0)$ is the viscosity evaluated at temperature T in the limit of zero pressure. (The sum of flows through N parallel identical capillaries is larger by a factor of N.)

B. Corrections to flow through a straight capillary

The large bracket in Eq. (1) contains five correction terms that depend on the Reynolds number Re, Knudsen number Kn, the aspect ratio R/L, and the pressure ratio P_2/P_1. Although the density dependence of viscosity causes Re to vary along the length of the capillary, a suitable definition that makes Re constant is

$$\text{Re} \equiv \frac{2M\dot{n}}{\pi R \eta(T, \bar{P})}. \tag{3}$$

Here the molar mass is M, and the pressure averaged along the length of the capillary is[3]

$$\bar{P} \equiv \frac{1}{L}\int_0^L P(z)dz \cong \frac{2}{3}\left(\frac{P_1^3 - P_2^3}{P_1^2 - P_2^2}\right). \tag{4}$$

The density dependence of viscosity is so weak, and the correction terms in Eq. (1) are so small, that using Eq. (3) to approximate Re by a constant is adequate. Table III gives the values of the coefficients used in four of the corrections in Eq. (1). The following subsections describe the five corrections for straight flow.

1. Deviations from the ideal gas law

The function g_{virial} accounts for deviations of the gas compressibility from the ideal gas law. In the present context, the gas density ρ is conveniently described by the second and third pressure virial coefficients, B_P and C_P, as follows:

$$\rho = \frac{M}{R_{\text{gas}}T}\frac{P}{(1+B_P P + C_P P^2)}. \tag{5}$$

(A deviation that increases the average density increases the flow rate.) The function g_{virial} also accounts for the density dependence of viscosity, which can be described by virial coefficients of viscosity, b and c, as follows:

$$\eta(T,\rho) \cong \eta(T,0)\left[1 + b\left(\frac{R_{gas}T\rho}{M}\right) + c\left(\frac{R_{gas}T\rho}{M}\right)^2\right] \tag{6}$$

(a deviation that increases the viscosity decreases the flow rate). The two density dependences combine as[4]

$$g_{\text{virial}}(P_1,P_2) \cong -(B_P+b)\overline{P} - [C_P + c - (B_P+b)^2] \times (P_1^2+P_2^2)/2. \tag{7}$$

2. Slip

The term proportional to K_{slip} corrects for slip at the capillary walls, which increases the flow rate.[9–11] This effect is proportional to the Knudsen number, defined by

$$\text{Kn} \equiv \frac{\lambda_{1/2}}{R} = \frac{1}{R}\left(\frac{2R_{\text{gas}}T}{M}\right)^{1/2}\frac{\eta_{1/2}}{P_{1/2}}, \tag{8}$$

where $\lambda_{1/2}$ is the mean free path at pressure $P_{1/2}$. (This definition is 1.1 times larger than that used in Ref. 3.) The "half" quantities are defined by

$$P_{1/2} \equiv \frac{P_1+P_2}{2}$$

and

$$\eta_{1/2} \equiv \eta(T,P_{1/2}). \tag{9}$$

The value $K_{\text{slip}}=1.0$, which represents complete momentum accommodation, likely describes most gases. This was verified by measuring the pressure dependence of flows of nitrogen, argon, propane, and sulfur hexafluoride.[4] Helium was an exception that required a value as large as $K_{\text{slip}}=1.2$. The use of helium in the QCFM requires a determination of K_{slip} from at least two measurements at the same flow rate but at different average pressures.

3. Changes of kinetic energy

The term proportional to K_{ent} corrects for the increase of kinetic energy that occurs near the capillary entrance.[7] The increase occurs because the average velocity of the gas increases as it flows into the entrance of the capillary. It increases further as the flow profile changes from nearly uniform at the entrance to nearly parabolic downstream. The resulting pressure drop decreases the flow rate. The term proportional to K_{exp} corrects for gas expansion along the capillary, which also increases the kinetic energy and decreases the flow rate.[8]

4. Viscous heating

The term proportional to K_{therm} accounts for the radial temperature distribution of the gas in the capillary, which results from the combination of heating due to friction and cooling due to gas expansion.[6] These two effects nearly cancel, so that the temperature of the gas in the middle of the capillary is slightly cooler than that of the wall. The coefficient for the thermal correction is

$$K_{\text{therm}}(T) = -\left[1 + \frac{1}{3}\left(\frac{T}{\eta}\frac{\partial\eta}{\partial T}\right)\right]\left(\frac{R_{\text{gas}}\eta}{M\kappa}\right), \tag{10}$$

where κ is the thermal conductivity.

C. Flow through a curved capillary

The third part of the model corrects for the centrifugal effects through the function $f_{\text{cent}}(\text{De}, R/R_{\text{curve}})$. Its arguments are the Dean number, defined by

$$\text{De} \equiv \text{Re}\left(\frac{R}{R_{\text{curve}}}\right)^{1/2}, \tag{11}$$

and the curvature ratio R/R_{curve}, where R_{curve} is the radius of curvature of the coil. Larrain and Bonilla[12] used a double series expansion to calculate f_{cent} for De$<$16. Their result can be approximated in simple form by

$$f_{\text{cent}}(\text{De},R/R_{\text{curve}}) \cong [1 + a_4\text{De}^4 + a_8\text{De}^8] \times \left[1 + \left(\frac{R}{R_{\text{curve}}}\right)\left(\frac{\text{De}}{\text{De}_0}\right)^2\right], \tag{12}$$

where $a_4 = -3.567\times10^{-7}$, $a_8 = +7.1\times10^{-13}$, and $\text{De}_0 = 40$. For the present flow meter, this approximation is valid to 0.01%, and for $R/R_{\text{curve}}<0.005$, it is valid to 0.02%. Reference 4 discusses flows where De$>$16.

Equation (1) neglects the ends of the coil where the capillary is straight. Accounting for the length L_{straight} of straight capillary included in the total length L modifies Eq. (1) as follows:

$$f_{\text{cent}} \Rightarrow \frac{L f_{\text{cent}}}{[L - L_{\text{straight}}(1-f_{\text{cent}})]}. \tag{13}$$

V. UNCERTAINTY

Equation (14) gives the total uncertainty of the QCFM. All values represent standard uncertainties (68% confidence, or a coverage factor $k=1$). Except for the pressure resolution δP, all of the uncertainties are "type B"[13]

$$\frac{u_{\text{flow}}}{\dot{n}} = \left[\left(4\frac{u_R}{R}\right)^2 + 4\left(\frac{u_P}{P_1+P_2}\right)^2 + 2\left(\frac{\delta P}{P_1-P_2}\right)^2 + \left(\left(\frac{\text{De}}{f_{\text{cent}}}\frac{\partial f_{\text{cent}}}{\partial \text{De}}\right)\frac{u_\eta}{\eta}\right)^2 + \Delta_T^2 + \Delta_x^2\right]^{1/2}. \tag{14}$$

Table IV gives the values of the parameters used in Eq. (14) that are independent of the flow rate. The normalized derivative of f_{cent} in the fourth term increases from 0 to -0.07 as De increases from 0 to 16. Table IV also gives a typical uncertainty budget. The total uncertainty is dominated by the uncertainty of the primary standards used to determine the capillary radius. Thus, except for small flows ($<$5% of the maximum for the flow element), the uncertainty for all three flow elements is approximately 0.03%.

The reproducibility of the QCFM is determined by variations of the lab temperature and the uncertainty and resolution of the pressure measurements because those quantities

TABLE IV. Uncertainty parameters in Eq. (14) and a typical uncertainty budget for 10 μmol/s of nitrogen through the medium flow element. All values are standard uncertainties (68% confidence).

Parameter		Value ($k=1$)	Relative flow uncertainty
capillary radius	u_R/R	0.00005	0.019%
pressure uncertainty	u_P	7 Pa	0.002%
pressure resolution	δP	1 Pa	0.005%
viscosity (N_2)[a]	u_η/η	0.003	0.000%
lab temperature (± 1 K)	Δ_T	0.000 10	0.010%
gas purity (99.99%)	Δ_x	0.000 10	0.010%
		Quadrature sum	**0.024%**

[a]See Ref. 14.

can vary between flow measurements. In Table IV, their quadrature sum predicts a reproducibility of 0.011%, which is similar to the rms scatter of 0.010% seen in Fig. 1 for the medium flow element (No. 5 $PVTt$). This means that Table IV does not neglect a significant random contribution to the uncertainty. The following subsections discuss the contributions to u_{flow}.

A. Capillary radius

The uncertainties of the primary flow standards u_{primary} dominate the uncertainty u_R of the effective radius R of the capillary. The standard uncertainty of both primary standards is $u_{\text{primary}}=0.019\%$,[2] and Fig. 1 shows that the primaries are in agreement. This leads to the estimate

$$\frac{u_R}{R}=\frac{1}{4}\frac{u_{\text{primary}}}{\dot{n}}=\frac{0.00019}{4}=0.005\% \tag{15}$$

for the relative uncertainty of R.

B. Other capillary lengths

The uncertainty of the capillary length L contributes negligibly to the flow uncertainty. An error in the value assumed for L merely shifts the effective value of R without changing the value of L/R^4.

The centrifugal correction depends on R, R_{curve}, L, and L_{straight}. The uncertainty of flow caused by the uncertainty of these lengths is negligible except for the value of L_{straight} at large De. The uncertainty of $u_{\text{Lstraight}}\approx 20$ mm contributed 0.02% to the uncertainty of the largest flow shown in Fig. 1.

C. Temperature

A temperature error causes a flow rate error because both gas density and viscosity depend on temperature. The average temperature of the flow element is assumed to be the average of the readings of the two thermometers in the air bath. Sources of temperature uncertainty are included in the following subsections.

1. Thermometer uncertainty

The uncertainty of the thermometers was estimated by placing them at a common location in the air bath. They agreed with each other and with an independent thermometer to within 0.01 K. The corresponding uncertainties in the gas density and viscosity at first seem to suggest a flow uncertainty as large as of 0.01%. Actually, the flow uncertainty is negligible because the flow measurements are made at the same temperature used to calibrate the effective radius of the capillary. (This assumes that any drift of the thermometers during the interval between the radius calibration and the flow measurement was negligible.)

2. Temperature differences in the air bath and variations of the laboratory temperature

Temperature differences within the air bath cause the average thermometer temperature T_{PRT} to differ from the true average temperature T of the flow element. The difference $T-T_{\text{PRT}}$ during a flow measurement is *not* a source of error if it is the same that occurred during the calibration of the effective radius. However, changing the laboratory temperature T_{lab} will change the temperature distribution of the air bath, which could change $T-T_{\text{PRT}}$. In addition, the temperature of the gas entering the capillary will differ from T if both $|T-T_{\text{lab}}|$ and the flow rate are sufficiently large. As a test, T_{PRT} was decreased from 25 to 15 °C, which increased the top–bottom temperature difference of the air bath from -0.18 to $+0.16$ K. However, the deviation of the modeled flow from the actual flow changed by only 0.1%, and only for $\dot{n}>1000\,\mu$mol/s. This result places a bound on the relative flow uncertainty due to room temperature. A 1 K shift of T_{lab} from the calibration temperature (22 °C) will contribute a flow uncertainty of less than $\Delta_T=0.01\%$.

D. Pressure

After the gauges were recalibrated, their uncertainties were limited by hysteresis and by the deviation of the gauge function from its description by a cubic polynomial. Both quantities were about 5 Pa; their quadrature sum yields the gauge uncertainty $u_P=7$ Pa. Pressure taring gives a special status to the pressure difference $P_-\equiv(P_1-P_2)$ by minimizing its uncertainty u_{P_-} when P_- is small. Therefore, it is useful to approximate the pressure dependence of the molar flow rate as

$$\dot{n}\propto(P_1+P_2)(P_1-P_2)\equiv P_+P_-. \tag{16}$$

The uncertainty of the pressure sum is approximately

$$u_{P_+}=\sqrt{2}u_P, \tag{17}$$

and the uncertainty of the pressure difference is approximately

$$u_{P_-}=\sqrt{2}\left[(\delta P)^2+\left(\frac{P_-}{P_{\text{full scale}}}\right)^2(u_P)^2\right]^{1/2}$$
$$\approx\sqrt{2}\left[(\delta P)^2+\left(\frac{P_-}{P_+}\right)^2(u_P)^2\right]^{1/2}. \tag{18}$$

The first term of Eq. (18) accounts for the resolution of the gauges ($\delta P=1$ Pa). The second term assumes that the systematic error of P_- scales with the full-scale pressure $P_{\text{fullscale}}$. The flow uncertainty due to pressure is thus

$$\left(\frac{u_{\text{flow}}}{\dot{n}}\right)_P = \frac{1}{P_+ P_-}\left[\left(\frac{\partial \dot{n}}{\partial P_+}\right)^2 u_{P_+}^2 + \left(\frac{\partial \dot{n}}{\partial P_-}\right)^2 u_{P_-}^2\right]^{1/2}$$
$$= \left[\left(\frac{u_{P_+}}{P_+}\right)^2 + \left(\frac{u_{P_-}}{P_-}\right)^2\right]^{1/2}$$
$$\cong \left[4\left(\frac{u_P}{P_+}\right)^2 + 2\left(\frac{\delta P}{P_-}\right)^2\right]^{1/2}. \quad (19)$$

For large flows, $P_1 - P_2$ is large, and the gauge uncertainty u_P dominates the pressure contribution to flow uncertainty. For flows less than about 5% of maximum, the resolution δP dominates.

E. Gas properties

Equation (1) for flow through a straight capillary does not require a highly accurate value for the viscosity of nitrogen because the calibration with nitrogen yields an effective radius for the capillary. Measuring the flow rate of a different gas requires knowledge only of the *ratio* of the gas viscosity to that of nitrogen. In contrast, the centrifugal correction does require an absolute value for viscosity. Equation (1) implies that the resulting flow uncertainty due to u_η is

$$\left(\frac{u_{\dot{n}}}{\dot{n}}\right)_\eta = \left|\left(\frac{\partial f_{\text{cent}}}{\partial \text{De}}\right)\left(\frac{\partial \text{De}}{\partial \eta}\right)\right| u_\eta$$
$$= \left|\frac{\text{De}}{f_{\text{cent}}}\frac{\partial f_{\text{cent}}}{\partial \text{De}}\right|\left(\frac{u_\eta}{\eta}\right)$$
$$< \frac{1}{4}\left(\frac{u_\eta}{\eta}\right). \quad (20)$$

The uncertainty of the published viscosity of nitrogen is $u_\eta/\eta = 0.3\%$.[14] For De<16, the contribution to the relative flow uncertainty is 0.021% or less.

The offsets of other gases from nitrogen seen in Fig. 2 are within the uncertainties of the ratios of published viscosity values. The offset values can provide more accurate viscosity ratios because they are independent of flow rate.[4]

In Eq. (1), the uncertainty of the virial correction function g_{virial} may be significant for gases such as SF_6 that have a large second pressure virial coefficient B_P. A recent careful study of the properties of SF_6[15] does not state the uncertainty of B_P directly; however inspection of deviation plots in Ref. 15 suggest that it is roughly 1% near 300 K. The resulting contribution to the flow uncertainty would be as large as $\Delta_B = 0.02\%$. The corresponding uncertainty for propane is likely larger.

F. Gas purity

The effect of impurities on gas viscosity is mild because the viscosity depends only weakly on composition. For example, among the five gases used here, the viscosity at 25 °C and 100 kPa varies by less than a factor of 3. For these and most other gases, the relative flow uncertainty caused by 99.99% purity is approximately $\Delta_x = 0.01\%$.

VI. DESIGN ALGORITHM

The design of each flow element required choices for the capillary radius R and length L, the entrance pressure P_1, and the number of capillaries N. (Convenience limited the assignments of temperature, exit pressure, and coil radius to the values $T = 25\,°\text{C}$, $P_2 = 100\,\text{kPa}$, and $R_{\text{curve}} = 100\,\text{mm}$.) This section gives six steps for choosing R, L, P_1, and N. In this example, the gas is nitrogen, the maximum flow rate is 1000 μmol/s, and the desired relative flow uncertainty is $\delta = 0.03\%$.

A. Define the minimum radius

Increasing the capillary radius decreases the uncertainty due to slip. The required minimum radius is therefore

$$R_{\min} = \frac{4\lambda_{\max} u(K_{\text{slip}})}{\delta}$$
$$= \frac{(4)(0.075\ \mu\text{m})(0.1)}{(0.0003)}$$
$$= 100\ \mu\text{m}, \quad (21)$$

where $\lambda_{\max}$ is the largest expected mean free path. The value of $\lambda_{\max}$ for nitrogen at atmospheric pressure is used here. The value of $u(K_{\text{slip}})$, the uncertainty of the slip correction, is based on the present work.

B. Define the maximum Dean number

The centrifugal correction based on Larrain and Bonilla's result is valid only up to

$$\text{De}_{\max} = 16. \quad (22)$$

Note that operating a coiled capillary flow meter at De>16 requires more than an accurate expression for f_{cent}. Imperfections of the capillary cross section, such as ellipticity and variations of the radius along the capillary length, must be sufficiently small to avoid significant error at large De.[4]

C. Calculate the maximum Reynolds number

The maximum Dean number implies a maximum Reynolds number given by

$$\text{Re}_{\max} = \text{De}_{\max}\sqrt{\frac{R_{\text{curve}}}{R_{\min}}} = 506. \quad (23)$$

This value is safely below the critical value for straight pipe flow, $\text{Re}_{\text{crit}} = 2300$.[7]

D. Define the minimum capillary length

Decreasing the capillary length increases the uncertainty of three of the corrections to Eq. (1). The most important of these is the entrance correction due to the large uncertainty $u(K_{\text{ent}})$ of its coefficient. After converting Re to De, one obtains from the entrance correction the required minimum capillary length

$$L_{\min} = \frac{u(K_{\text{ent}})\text{De}_{\max}\sqrt{RR_{\text{curve}}}}{16\delta} = 1.05\ \text{m}. \quad (24)$$

The uncertainty $u(K_{\text{ent}})=0.1$ was estimated from the spread of values reported in Ref. 7.

E. Define the maximum entrance pressure

The maximum entrance pressure $P_{1\,\max}$ is determined by the maximum Reynolds number, which also determines the maximum flow rate through a single capillary $\dot{n}_{\max}$. Solve Eq. (2) for P_1 and use Eq. (3) to write $\dot{n}_{\max}$ in terms of $\mathrm{Re}_{\max}$. The result is

$$P_{1\,\max}=\left[\frac{8\,\eta^2 L_{\min} R_{\text{gas}} T\,\mathrm{Re}_{\max}}{M R_{\min}^3}+P_2^2\right]^{1/2}=360\ \ \text{kPa}. \quad (25)$$

F. Define the number of capillaries

Multiple capillaries in parallel are required if $\dot{n}_{1\,\max}$ exceeds the maximum flow rate through one capillary $\dot{n}_{1\,\max}$. For this example, the required number of capillaries is

$$N=\frac{\dot{n}_{\max}}{\dot{n}_{1\,\max}}=\frac{\dot{n}_{\max}}{\left(\dfrac{\pi\eta R_{\min}\mathrm{Re}_{\max}}{2M}\right)}=\frac{1000\ \ \mu\text{mol/s}}{51\ \ \mu\text{mol/s}}\approx 20. \quad (26)$$

ACKNOWLEDGMENTS

Mike Moldover encouraged this work with his constant interest and he pointed out a useful approximation for g_{virial}. John Hurly provided information about gas properties, Arno Laesecke identified much of the literature on centrifugal effects, and Jim Schmidt provided the propane. Jeff Kelley suggested the removable frame. Pierre Delajoud, Tom Maginnis, and John Wright gave further stimulation and help. This investigation originated in Stuart Tison's design of and measurements with the stainless steel transfer standard. The work was supported by the NIST Semiconductor Metrology Program.

[1] R. F. Berg and G. Cignolo, Metrologia **40**, 154 (2003).
[2] R. F. Berg and S. A. Tison (unpublished).
[3] R. F. Berg and S. A. Tison, AIChE J. **47**, 263 (2000).
[4] R. F. Berg, J. Res. NIST (2004).
[5] Certain commercial equipment, instruments, or materials are identified in this article to foster understanding. Such identification does not imply recommendation or endorsement by the National Institute of Standards and Technology, nor does it imply that the materials or equipment identified are necessarily the best available for the purpose.
[6] H. R. van den Berg, C. A. ten Seldam, and P. S. van der Gulik, Int. J. Thermophys. **14**, 865 (1993).
[7] M. Kawata, K. Kurase, A. Nagashima, and K. Yoshida, *Capillary Viscometers*, Chapter 3, Measurement of the Transport Properties of Fluids, edited by W. A. Wakeham, A. Nagashima, and J. V. Sengers (Blackwell Scientific, London, 1991).
[8] H. R. van den Berg, C. A. ten Seldam, and P. S. van der Gulik, J. Fluid Mech. **246**, 1 (1993).
[9] E. H. Kennard, *Kinetic Theory of Gases* (McGraw–Hill, New York, 1938).
[10] A. L. Thomson and W. R. Owens, Vacuum **25**, 151 (1975).
[11] F. Sharipov and V. Seleznev, J. Phys. Chem. Ref. Data **27**, 657 (1998).
[12] J. Larrain and C. F. Bonilla, Trans. Soc. Rheol. **14**, 135 (1970).
[13] B. N. Taylor and C. E. Kuyatt, NIST Tech. Note , 1297 (1994).
[14] W. A. Wakeham and W. A. Cole, J. Phys. Chem. Ref. Data **14**, 209 (1989).
[15] J. J. Hurly, D. R. Defibaugh, and M. R. Moldover, Int. J. Thermophys. **21**, 739 (2000).